Scientific Research Publishing

Journal of Geoscience and Environment Protection, 2026, 14(8), 1-21
https://www.scirp.org/journal/gep
ISSN Online: 2327-4344
ISSN Print: 2327-4336

Geological Structural Mapping Using Aeromagnetic Geophysical Data: A Case of Winneba and Its Environs, Central Region, Ghana

Daniel Oduro Boatey Nuamah

Department of Geological Engineering, Faculty of Civil and Geo-Engineering, College of Engineering, Kwame Nkrumah University of Science and Technology, Kumasi, Ghana
Email: danielobnuamah54@gmail.com

How to cite this paper: Nuamah, D. O. B. (2026). Geological Structural Mapping Using Aeromagnetic Geophysical Data: A Case of Winneba and Its Environs, Central Region, Ghana. *Journal of Geoscience and Environment Protection, 14,* 1-21.
https://doi.org/10.4236/gep.2026.148001

Received: June 11, 2026
Accepted: July 28, 2026
Published: July 31, 2026

Abstract

The aeromagnetic geophysical survey method has been applied to the Winneba area, south-eastern Ghana, to map geological structures, lithological contacts and measure the thickness of the overburden materials for mineral exploration purpose. The Centre for Exploration Targeting (CET) Grid Analysis was applied with the edge detection filters to map lineament positions while the Source Parameter Imaging (SPI) technique was used to measure spatial depths to the crystalline basement rocks at various locations to estimate overburden material thickness. The processed magnetic field intensity anomalies categorized the geology of the study area into metamorphosed sedimentary, volcaniclastic and volcanic rocks. Mapped geological contacts separating the different rock types were interpreted as boundaries of interest for mineralization. The delineated geological structures were major and minor dykes associated with volcanic intrusives. Estimated depths to the underlying hard rocks showed variations in material thickness over the study area. Deeper depth areas greater than 300 m occur to the southeast while shallower depth areas less than 150 m, were positioned along surficial mapped dykes. An intermediate depths range of 150 m-to 300 m were measured at several locations across the study area. The highest estimated depth is 753 m, located southeast, closer to the shoreline. The variations in depth measurements indicated the overburden material is thicker to the southeast compared to other parts of the study area. The mapped litho-contacts and intrusive dyke locations are proposed zones for possible mineral accumulation, hence, further exploration activities should target these areas.

Keywords

Geological Structure, Depth Measurements, CET Grid Analyses, Source Parameter Imaging

1. Introduction

The geophysical field of study has improved technology and theoretical foundation in operational methods such as gravity, electromagnetic, radiometric, induce polarization, magnetic and seismic. These field operational techniques measure different earth physical properties and applied to different engineering scenarios. They are distinguished by their field principles and survey procedures. Measured earths physical parameter such as rock density, magnetic field intensity, electrical resistivity and radioactivity are interpreted to delineate earth resources (Lowrie, 2007). Geophysical methods are not invasive and destructive techniques and hence, used to assess the conditions of the earth by measuring changes in its physical parameters (Kovačević et al., 2018). The magnetic properties of earth materials create anomalous zones in the earth's magnetic field which can be recorded by an aeromagnetic geophysical field survey for geological interpretation. The theoretical foundation of the magnetic method relies on induced magnetization of rocks. Measured total magnetic field intensity is an addition of the regional background magnetic field and the induced magnetic susceptibility field originating from earth materials. The magnetization of different rock types which is directly related to their levels of magnetic minerals is the bases for charactering the different rock units (Telford et al., 1990). A field magnetic survey was conducted across the study area to acquire data for this research. Recent mineral exploration activities target deposits at depth where the traditional prospecting methods such as geochemical field analysis and geological field mapping are limited. This is because they give point data and have a shorter depth of penetration. At instances where a higher depth of investigation is required, the traditional methods have proven to be inconclusive in certain instances and also expensive. Geological structures of importance in mineral exploration are occasional buried at depth, hence, the need for a method to investigation deeper depths to map these structures (Akulga, 2013). The aeromagnetic method was used in this study because of its deeper depth of investigation and its ability to produce a continuous data. The method is efficient in establishing the spatial extent of rocks, mapping deeper geological structural positions and estimating overburden thickness (Nabighian et al., 2005). The data is processed, analyzed and interpreted using standard geophysical filters to improve geological structural features that are not accessible in field geological mapping (Nabighian et al., 2005; Ilesanmi et al., 2025). The aeromagnetic geophysical method was used in this research to map the lateral extent of rocks, geological structural positions and estimate the thickness of overburden materials for mineral exploration purposes. Linearized structures such as dykes, shear zones, faults and litho-contact were mapped using the CET Grid analyses applied to the horizontal, vertical and tilt derivatives of the total magnetic field intensity. The Source Parameter Imaging (SPI) method was used to measure spatial depth to magnetic sources across the survey area (Ilesanmi et al., 2025), revealing the overburden thickness.

1.1. Geology and Tectonic Settings

The study area form part of two major litho-tectonic settings and have experienced several tectonic activities. It is situated on the southern coast of Ghana and forms part of the Kibi-Winneba volcanic belt, belonging to the Paleoproterozoic Birimian Supergroup of the West African Craton (WAC) and the Dahomeyan basement rocks of the Dahomeyide belt, Southeastern Ghana, belonging to the Neoproterozoic Trans-Saharan Shear Zone, West Africa. The Birimian terrane is a younger crust formed approximately 2.2 - 2.1 Ga during the Paleoproterozoic Era (Hirdes et al., 1992). The Birimian rocks were changed as a result of the Eburnean orogenic event, which is the main tectono-magmatic orogenic event responsible for the re-structuring of the Birimian area. The Birimian Supergroup is widely emplaced across Ghana and the entire West African subregion. It is made up of metamorphosed volcanic and sedimentary units intruded by granitic rocks. The Birimian terrane is part of the eastern segment of the West African Craton known as the Leo-Man Shield (Taylor et al., 1992). The rocks are configured in a belt-basin geometry, thus, metavolcanic belts known as the greenstones are separated by metasedimentary basins. The Kibi-Winneba belt is a southeastern Birimian belts in Ghana covering parts of the Winneba area. The belt is oriented in the northeast-southwest direction, which matches the regional structural trend of Birimian terranes in West-Africa (Forson et al., 2020). The belt covers parts of the Eastern and Central Regions of Ghana, with the Kibi municipality to the north and the coastal town of Winneba to the south. Lithologically, the Kibi-Winneba belt contains metavolcanic rocks, metasedimentary units and intrusive granitoids. The metavolcanic rocks are predominantly mafic (basalts) to intermediate (andesites) in composition, while the metasedimentary units consist mainly of greywacke, shale and volcaniclastics (Pigois et al., 2003). Granitic intrusives are common all over the Birimian terrane. The granitic rocks in the Kibi-Winneba belt show volcanic-arc geochemical signatures. They evolved from crustal melting as a result intensive thermal activity associated with the Eburnean orogenic event (Anum et al., 2015). They are composed of tonalites and granodiorite intruding the metamorphosed volcanic and sedimentary units. Structurally, the rocks of the Kibi-Winneba belt are characterized by faults, folds and shear zones formed during Eburnean deformational event. The geological structural configuration is a factor that controls mineralization and fluid accumulation in the belt. Forson et al. (2021) stated that the main areas of mineralization in the belt are tectonized shear contacts and fracture networks. The belt hosts quartz veins and sulphide gold mineralization similar to other Birimian belts. Mesothermal gold deposits occur with arsenopyrite and pyrite as pathfinders formed from hydrothermal fluids accumulated in shear contacts (Groves et al., 2003).

The Trans-Saharan Shear Zone is an important Pan-African tectonic belts in West Africa. It runs in a broadly north-northeast to south-southwest direction along the eastern margins of Ghana, Togo and Benin through to southwestern Nigeria. This belt marks the collisional zone formed during the Pan-African orogeny, a period of continental convergence that occurred around 600-550Ma during the late Neoproterozoic Era (Affaton et al., 1991; Castaing et al., 1993). The southern part of the Pan-African Trans-Saharan Shear Zone which occur in Ghana is known as the Dahomeyide belt. The Dahomeyide belt resulted from the collision of existing rocks of the West African Craton (WAC) in the west, with the rocks of the Nigeria-Benin Shield to the east. This resulted to a westward subduction of oceanic crust and the emplacement of high-grade metamorphic and granitic rocks along the collisional margin (Attoh et al., 1997). The belt is structurally divided into three major litho-tectonic zones that are characterized by deformation and metamorphic conditions from west to east. The western zone, made up of low-grade deformed marginal sediments of the Voltaian Basin consisting of metasedimentary rocks which are folded and faulted. The central suture zone, hosts high and ultra-high-pressure rocks of mantle origin including serpentinites, peridotites, amphibolies and eclogites. Also present are highly metamorphosed rocks of granitic origin made up of nepheline syenite gneisses, garnet gneisses and sericite gneisses (Attoh et al., 1997; Ganade et al., 2016). The eastern zone is covered by high-grade gneisses, migmatites and granulites of the rejuvenated passive margin rocks of the Nigeria-Benin Shield, that experienced deformation and high-grade metamorphism during the collision.

1.2. The Study Area

The study area (**Figure 1**) is Winneba and its environs in the Effutu Municipality, Central Region of Ghana. The town Winneba lies approximately 65 km southwest of Accra, the national capital and 50 km east of Cape Coast, the Regional Capital. Geographically, the study area is bounded by latitudes 5˚18'N to 5˚28'N and longitudes 0˚32'W to 0˚42'W covering an area of roughly 200 km^2 that encompasses some coastal towns with immediate inland communities. Geologically, the area falls within the transition between the Kibi-Winneba belt of the Birimian Supergroup and the Precambrian basement rocks of the Dahomeyide belt with a Quaternary coastal sedimentary cover. Access to the area is primarily via the "N1" coastal highway connecting the national capital, Accra to Cape Coast, the regional capital with secondary roads extending inland toward the surrounding communities. The Winneba area is generally low-lying, with elevations ranging from sea level to approximately 80 m above mean sea level. The terrain is predominantly flat to gently undulating, becoming more dissected northward where resistant metamorphic and granitoid lithologies exert greater topographic control. The coastline to the south of the study area is irregular and characterized by sandy beaches. Extensive areas of coastal scrub, thicker vegetation and secondary bushes cover much of the study area, significantly limiting geological exposures and accessibility to the bedrock. This dense vegetation cover, combined with thin lateritic soils and a coastal sediment blanket, substantially restricts the effectiveness of conventional surface geological mapping and provides a primary justification for the application of aeromagnetic methods in this study. Settlement patterns in the study area reflect a coastal-inland dichotomy, with dense nucleated settlements along the coastline and smaller dispersed farming communities distributed across the inland portions of the study area.

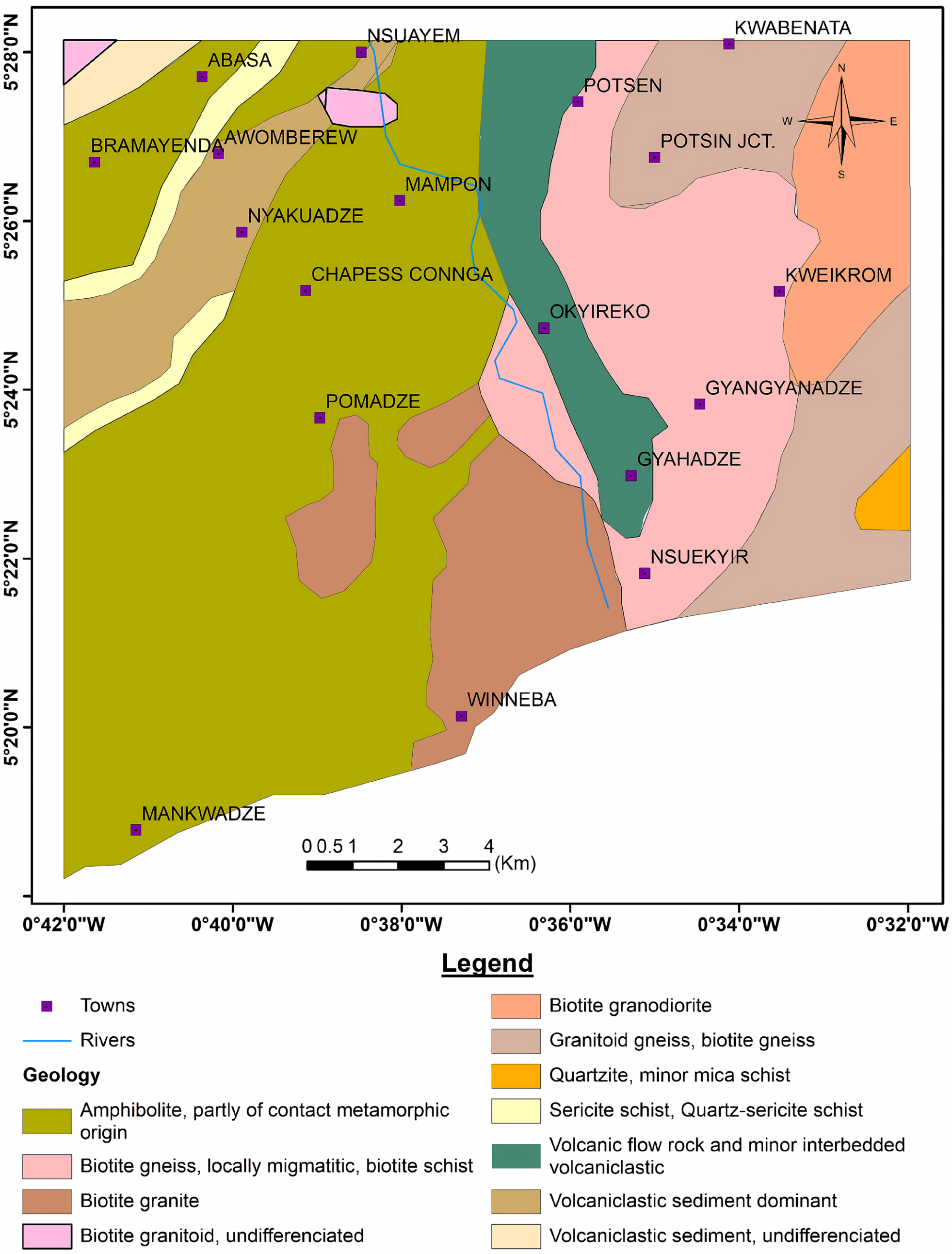

Figure 1. The geological map of the study area.

2. Materials and Methods

2.1. Magnetic Field Data Acquisition

Field surveyed aero-magnetics data was used for this research. The data used for this research was obtain from the Geological Survey Authority of Ghana. It was acquired in the year 2000 by High Sense Geophysics Incorporation, Canada. The initial field survey (Figure 2) was designed on equal survey line intervals to form a linearly spaced grid of 400 m at an angle of 315˚ with the supporting tie lines spaced at 5000 m intervals at 045˚ orientation. The data was acquired along the planned survey lines across the strike of the various lithologies using a proton precession magnetometer onboard an airplane flying at a nominal terrane clearance of 80 m. A total area of 200 km^2 was covered by the survey flight at a Nominal Airspeed 100 km/hr. Flight drift and tilt which are data errors associated with the flight path were corrected. These flight discrepancies are as a result of cross wind and wrong flight maneuvering. The final Magnetic Field Intensity (TMFI) comprising of the regional and residual fields were measured for further processing.

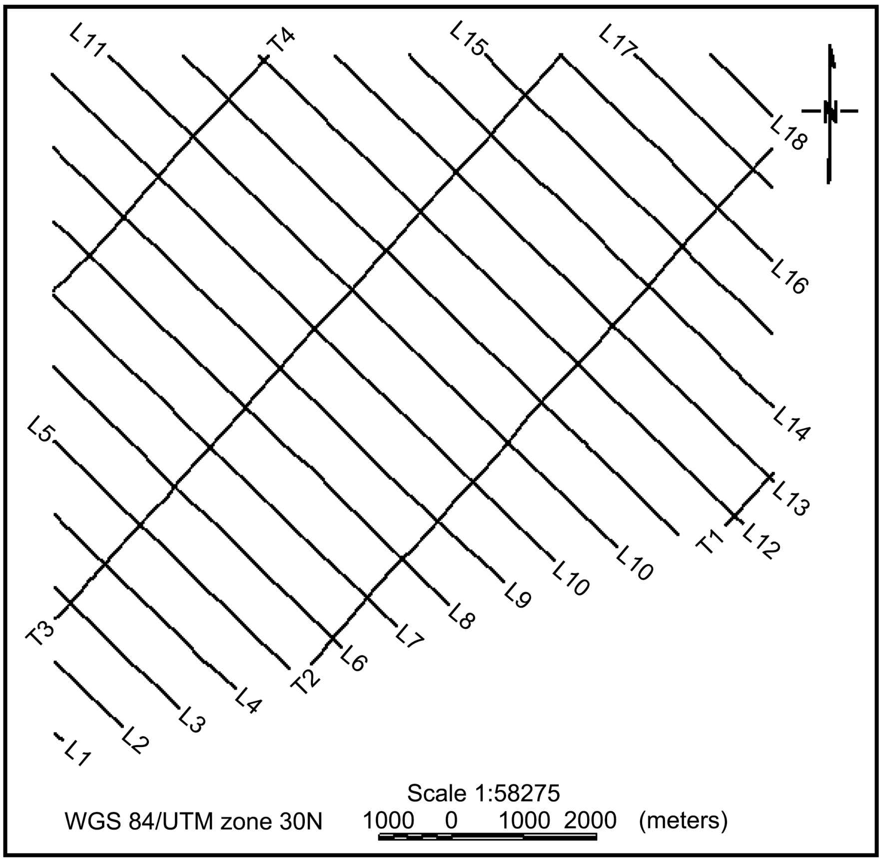

Figure 2. Aeromagnetic field survey grid lines.

2.2. Magnetic Data Processing

Magnetic data preprocessing which include a number of data reduction procedures were applied to the acquired data using the Geosoft Oasis Montaj software.

The data was edited to remove data spike values which are inconsistent with the data distribution. Magnetic field noise originating from cultural feature were also corrected. The resulting data contained only relevant magnetic field information from the rock's distribution in the study area. Further processing steps applied are data checking, diurnal changes removal, tie line leveling, geomagnetic reference field correction and micro leveling. The data was gridded using the minimum curvature estimation grid method with a grid cell size 100 m considering a one-quarter value from a field survey interval of 400 m. The result was a Total Field Intensity grid map showing the variation of magnetic field across the study area. Using an inclination and a declination values of -13° and -6° respectively at the time the field survey was conducted, the total field intensity was reduced to the equator to produce the true anomalous distribution in the study area. To enhance various geological features, interpretative grids such as Analytical Signal grid, Horizontal derivative, Vertical derivative, tilt derivative and their corresponding shaded intensity grid maps were produced. The robust CET Grid analyses and the Advanced Source Parameter Imaging technique were applied to analyze for lineaments and calculate relative depths to magnetic sources. The CET Grid analyses combine the edge detection filters to develop an integrated lineament system devoid of human influence.

2.3. Centre for Exploration Targeting (CET) Grid Analysis

The Advanced CET Grid Analysis was used to map linear features using the edges detection derivatives of the total magnetic intensity grid as input. The analyses are done automatically by delineating all possible lineament in all directions across the basement. The processing steps include Lineation detection, Amplitude thresholding and Lineament Vectorisation. Lineation detection delineate geological edges in field data irrespective of the field intensity orientation. The Amplitude thresholding procedure involve finding and mapping the linear thresholds which are the highest amplitudes in the grid. Mapped directional lines are then placed on the delineated linear thresholds through the process of Lineament Vectorisation. This automated lineament mapping tool is very robust such that all minor lineaments are approximated to aid in interpretation. Geological edge locations are indicative of magnetic intensities associated with magmatic intrusions which normally contain higher magnetic minerals. The CET Grid Analysis method maps geological edges on local magnetic intensity maximums and connects the output to symmetry locations within its immediate area. Lower magnetic field intensity measurements are suppressed while higher magnetic field intensity measurements are enhanced using the amplitude thresholding filter. The amplitude thresholding filter apply a maximal enhancement filter (NMF) to evaluate the data to determine the highest regions. The final delineated edges are emplaced using a skeletonization filter. This filter repeatedly joins boundary cells by connecting grid cell with mapped lineaments. The traditional edges detection methods which are horizontal, vertical and tilt derivative grids were used as an input data for the CET

Grid Analysis. The delineated lineaments were further interpreted as faults, dykes and lithologic contacts. Magnetic intensity maximums of horizontal derivative grids occur above geological litho-contacts while that of vertical derivative grids occur at fractured contacts such as faults. These same edges are mapped by marking the contacts of magnetic intensity highs and lows by the tilt derivative filter. The horizontal derivative of a magnetic field intensity is calculated from the equation:

$$HD(X,Y)=\sqrt{\left(\frac{\mathrm{d}M}{\mathrm{d}X}\right)^2+\left(\frac{\mathrm{d}M}{\mathrm{d}Y}\right)^2} \tag{1}$$

where "*HD*" is the horizontal derivative, $\left(\frac{\mathrm{d}M}{\mathrm{d}X}\right)$ is the "*x*" derivative of the measured field "*M*" and $\left(\frac{\mathrm{d}M}{\mathrm{d}Y}\right)$ is the "*y*" derivative of the measured field "*M*". The above equation gives the highest location above magnetic anomalies where the regional magnetic field is vertical, the magnetizations are vertical, the contacts are vertical, the contacts are isolated and the sources are thicker (Phillips, 1998). The challenge with vertical derivative filter is magnetic intensity peak shifts and the creation of additional peaks which has the capacity to mask true contacts. The vertical derivative is calculated by Equations (2):

$$VD=\mathrm{d}M/\mathrm{d}Z \tag{2}$$

where $\mathrm{d}M/\mathrm{d}Z$ is the derivative of the magnetic field "*M*" in the *Z*-direction. Miller and Singh (1994) also showed that, the tilt derivative crosses through zero contours at or near the edge of a vertical-sided source and is negative outside the source region. The tilt derivative is therefore very effective in allowing anomalies to be traced out along strike. According to Verduzco et al. (2004), the generalized tilt derivative equation is given as:

$$TD=\tan^{-1}\left(\frac{VD}{HD}\right) \tag{3}$$

where VD is the first vertical derivative of the measured field (*M*) and HD is the horizontal derivative. Thus, the tilt derivative is the ratio of the vertical derivative to the absolute amplitude of the total horizontal derivative of a magnetic field. Substituting Equations (1) and (2) in Equation (3) gives Equation (4);

$$TD=\tan^{-1}\left[\frac{\mathrm{d}M/\mathrm{d}Z}{\sqrt{(\mathrm{d}M/\mathrm{d}X)^2+(\mathrm{d}M/\mathrm{d}Y)^2}}\right] \tag{4}$$

2.4. Source Parameter Imaging (SPI)

Thurston and Smith (1997) theorized the mathematical basis for a spatial depth estimation method known as the Source Parameter Imaging (SPI). It is an automatic estimation procedure which require minimal human interface. The method uses the local wavenumber of the analytic signal grid to determine peak for depth value estimation. The analytical signal grid is calculated from the total magnetic intensity field grid. The rate of change of the local wavenumber spatially, is associated with the spatial distribution of magnetic anomalies, anomaly geometry and their depth of occurrence. The procedure maps peak positions from the analytical signal grid using higher wavenumbers over magnetic sources. the calculated peak value is inversely proportional to the depth interval to the anomalous body (Thurston & Smith, 1997). The depths measurements are then calculated from the local wavenumber at each grid vertices without prior information about the anomalies source locations, producing a spatially isolated relative depth grid map. The mathematical foundation of the ASPI is based on the relationship between the local wavenumber "k" and the sources depth "z", given by;

$$z = n/k \tag{5}$$

where "n" is the structural index resulting from the shape of the anomalous source body (Smith et al., 1998). A Structural index values of 0.5, 1, and 2 correspond to geological contacts, dykes and pipe type geometric shapes bodies respectively. A structural index value 1 was used for the SPI analyses to model depth solutions along higher magnitude such as dykes. The ASPI technique is efficient for estimating depths to the magnetic source from spatial gridded data than distinct line field surveys (Hinze et al., 2013). The ASPI Method is able to estimate precise depths without recourse to the direction of the inducing magnetic field which is advantageous over the traditional depth estimation methods. The purely induced magnetization concept is rooted in self-directional magnetization and the use of the analytic signal grid as the basal grid for depth estimation by the ASPI Method fulfill the fundamental basis for this theory (Nabighian, 1972). Comparing to the traditional derivative-based depth to magnetic sources estimation methods, the ASPI Method is not affected the inclination and declination of the total magnetic field making it a robust technique for mapping spatial depths.

3. Result and Interpretation

3.1. 2D Profile Models

Two-dimension anomaly models along the field survey lines were produced from the dataset (**Figure 3**). This was to assess the changes in magnetic intensities with associated anomalies in higher and lower intensities. An interactive bilinear method was used to model the field intensities along a y-axis with the field survey intervals on x-axis. The data was automatically inverted to produce a 2D-model for analyses. An Iterative inverse modelling approach was applied to model magnetic anomalies along survey lines using the Oasis Montaj software. This technique uses an automated routine to determine the adjustment to be made to the model parameters. The survey lines L4, L7, L9, and L14 were selected arbitrary to distribute the model profiles approximately equally across the study area. The Input parameters were the magnetic inclination, declination and the magnetic field background value at the time the data was taken. A magnetic field intensity data along a particular survey line is then chosen for modelling. Using the background field intensity value as an initial modelling parameter value, the inversion program conducts a number of iterations to determine the magnetic anomalies along the survey line. With a threshold anomalous values of zero (0) nanotesla, the modelled magnetic anomaly values range between +/− 250 nT. Figure 3(a) shows a 2D profile model along survey line "L4". The line covers a survey interval of 7341 m. A high magnetic anomaly was modeled along the entire stretch of this survey line. The highest anomaly observed was 160 nT which occur at the survey location 3500 m. The modelled anomaly profile dips at locations 700 m, 2500 m, 3600 m with positive anomaly values of approximately 1 nT, 40 nT and 80 nT respectively. Figure 3(b) shows the modelled profile line "L7" along a 6510 m interval. The first 2000 m continuous interval and the last 3510 m survey length showed an intermediate high magnetic anomaly of approximately 100 nT. An extremely low anomaly of −200 nT occurring at location 2700 m is followed by a high anomaly of 230 nT at survey location 2900 m. There are established geological contact at the zero (0) anomaly boundary from higher anomaly to lower anomaly and vice versa. The modelled profile, Figure 3(c) for line "L9", also demonstrated continuous intermediate high anomaly intensities along most of the survey length. The 7341 m line interval showed a middle lower anomaly, an intermediate and a high anomaly with measured field anomalies ranging from −150 nT to 150 nT. The highest anomaly value occurs at survey location 110 m with a measured positive anomaly value of 150 nT. The change in anomaly direction from high to low at location 3600 m boundary and low to high at location 3950 m boundary, shows a geological contact between two rock types in the study area. Figure 3(d) shows the changes in magnetic anomalies values along survey line "L14". The survey line covers a 2652 m interval and shows a continuous high anomaly at both ends of the modeled profile with a lower magnetic anomaly in between them. At an interval range of 0 - 2250 m, a high positive anomaly value of 1 - 100 nT is recorded.

This is followed by a low anomaly of −100 nT at survey location 2300 m. A litho-contact occurs at the various transitions from high to low and low to high anomalies positions. A review of the modeled anomaly distribution along the profiles to the geology of the Winneba area, indicates the observed high magnetic anomaly areas correlates with the onshore solid basement rocks of the Dahomeyide belt which are mostly granitic gneisses with higher magnetic minerals. The measured lower anomalies corresponded to areas occupied by the overlying metasedimentary rocks of the Birimian Supergroup which are mostly meta-arenites and meta-argillites. The modeled intermediate anomalies lie between metavolcanics and metasedimentary rocks. Their magnetic anomaly signature shows a mixture of metavolcanics and meta-clastic rocks of the southeastern Dahomeyide and the Birimian rocks, hence, are interpreted as volcaniclastics. Theoretical knowledge of the study area shows geological contacts between the metavolcanics, volcaniclastics and the metasedimentary rocks.

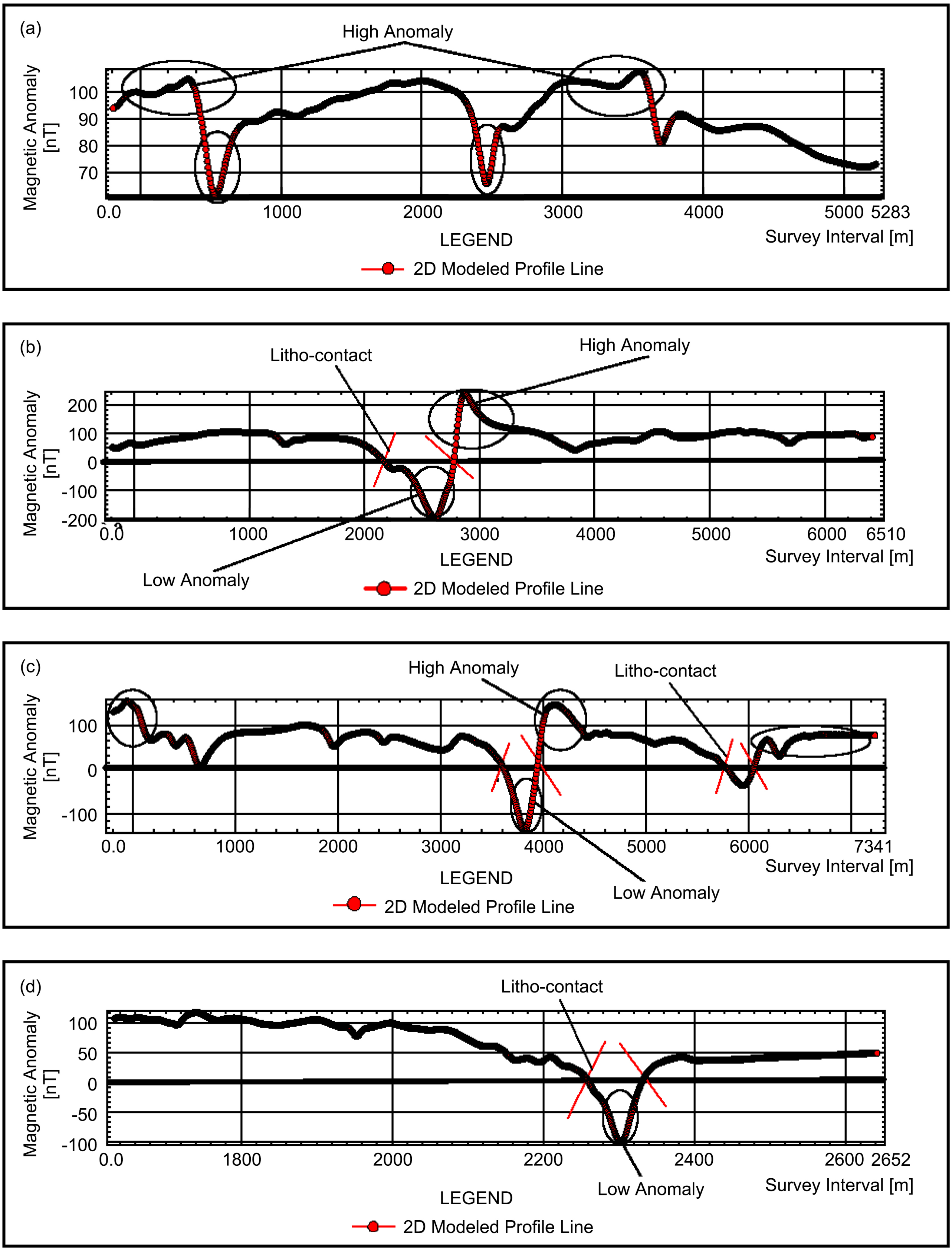

Figure 3. 2D profile models (a) Line "L4" (b) Line "L7" (c) Line "L9" (d) Line "L14".

3.2. 2D Grids Interpretation

3.2.1. Total Magnetic Intensity Grid (TMI)

A total magnetic intensity grid (Figure 4) was produced from the dataset. The induced magnetization of rocks is characterized by the remnant magnetization and the field magnetization from the earth's core. This include a residual and regional magnetic field intensity relating to the total magnetic field intensity. This shows the lateral distribution of the magnetic intensities in the study area. Higher intensities are indicated in red to magenta colours while lower magnetic intensities are shown in blue to green colours. The variations in the magnetic intensities is associated with the magnetization of the study area rocks. The position of Ghana is closer to the geographic equator and hence, the measured magnetic field intensities are overturned and shifted from their causative rocks, causing higher anomalies in blue colour to appear as lower anomalies and vice versa. As a result of this natural inversion of the magnetic field anomaly intensities, the crustal magnetization which are very strong occur to the southeast while weaker magnetizations occur to the northeast of the study area. The magnetic intensities measured ranges from 3 nT to approximately 125 nT. The observed magnetic intensities are from the differences in remnant magnetization of the overlying meta-sediments and the highly magnetic basement rocks.

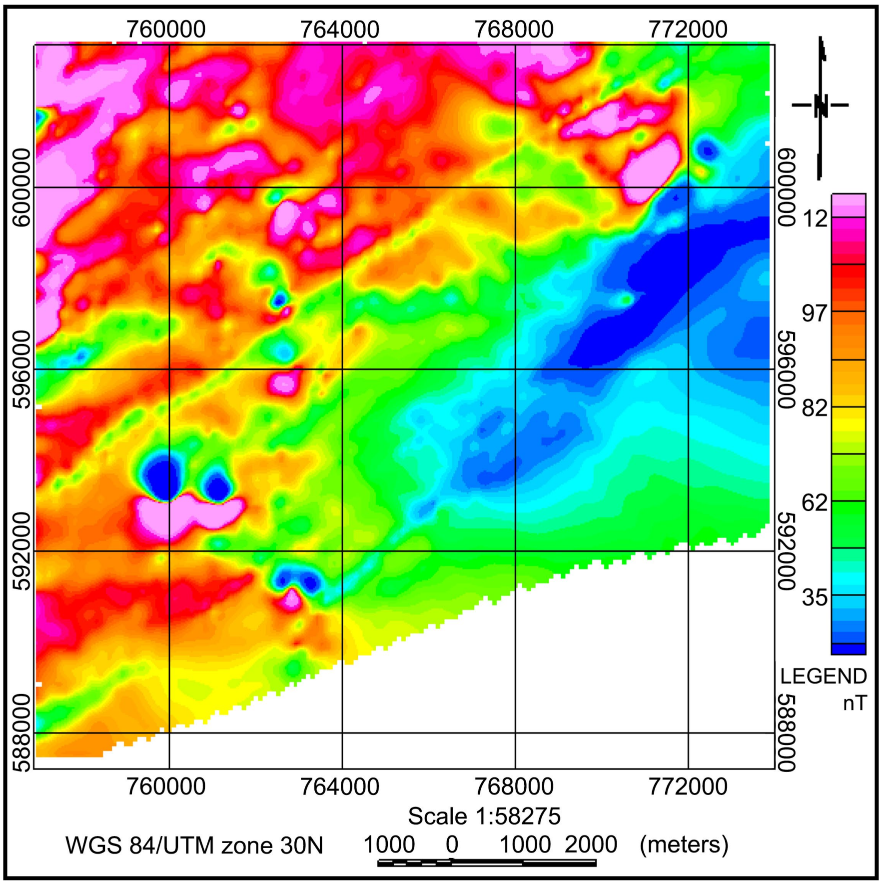

Figure 4. Total magnetic intensity (TMI) grid map of the study area.

3.2.2. Analytical Signal Grid (AS)

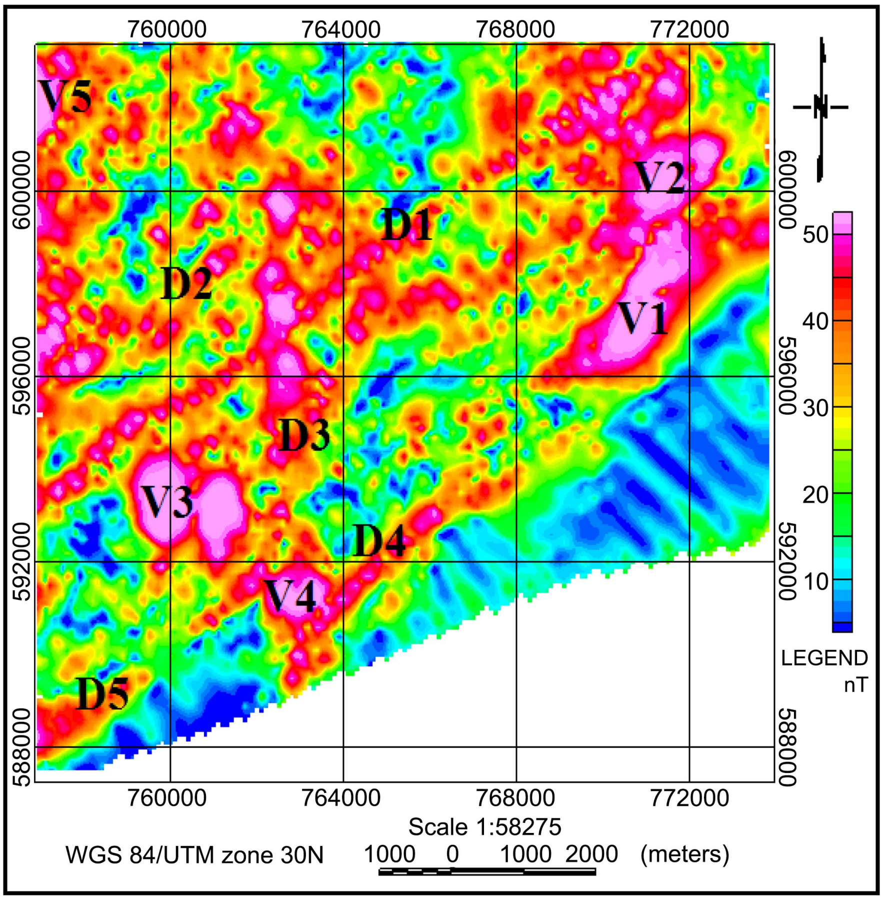

Figure 5. Analytical signal grid maps of the study area.

The total magnetic field intensities grid was further processed using the analytical signal filter (Figure 5) to show the lithological variation in the study area. This was to position the observed field magnetic anomalies directly on their subsurface magnetic rocks. The analytical signal filter is well suited for eliminating the disparities in magnetic anomaly position within lower geographical latitudes. The location of Ghana makes it an ideal filter for identifying exact magnetic anomaly position for interpretation. The observed magnetic anomaly intensities range from −3 nT to 53 nT. Higher magnetic anomaly intensities occur as lineaments throughout the study area and are related to intrusive volcanic dykes partly associated with magmatic igneous rocks of the Birimian tectonic settings. These linearized bodies occurring as dykes labelled "D1" to "D5" are oriented in the northeast-southwest direction. Their trend is consistent with the general lineament trend of the Birimian tectonic settings. The magmatic igneous rocks are shown as patches labelled "V1" to "V5" of high magnetic anomaly intensities in magenta colours. To the south, toward the sea are sedimentary cover rocks indicated in lower magnetic anomaly intensities in blue colour. These are mostly particulate sand and silt size rocks along the shore line. Some intermediate signatures in green colour are scattered throughout the study area mostly around the higher magnetic anomaly intensity metavolcanic rocks. It is related to the metamorphosed volcaniclastics rocks accumulated from volcanic ash and the breakdown of the metavolcanics in the study area. The analytical signal anomaly intensity distribution was effective in distinguishing the rock types and also revealed deep seated magnetizations which could not be assessed on the surface.

3.2.3. CET Analyses

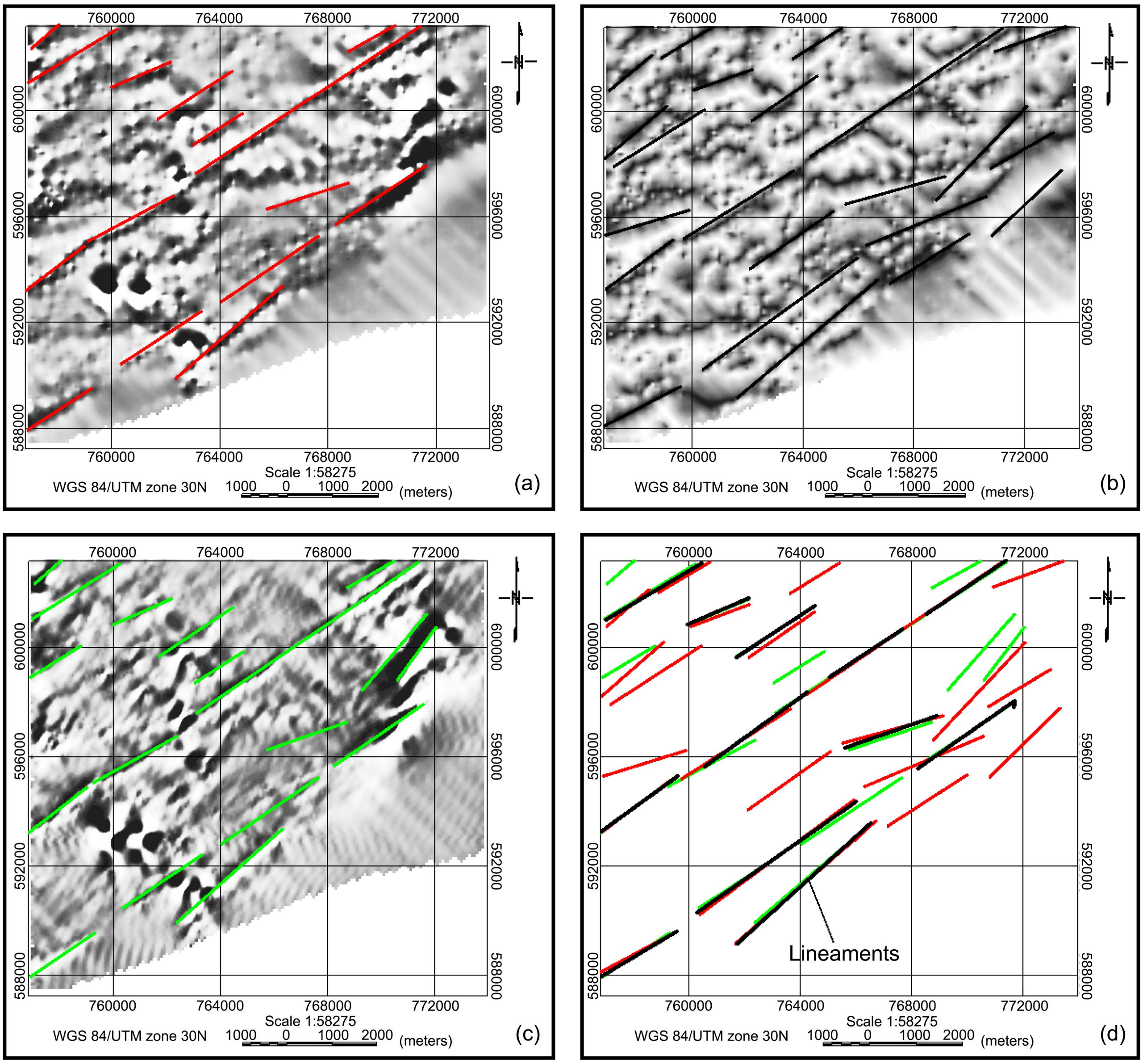

Figure 6. Mapped edge detection grid maps of the study area (a) Horizontal derivative (b) Vertical derivative (c) Tilt derivative (d) Composite lineaments map.

The study used the robust center for exploration targeting analyses to map out linearized structures in the research area. The method includes the Lineation detection, Amplitude thresholding and lineation vectorisation which assesses the survey area in smaller grid cells to locate magnetic intensities ridges to be mapped. These filters were applied to the edge detection method such as the horizontal, vertical and tilt derivatives (**Figure 6**). The edge detection methods initially derive the derivative of the absolute magnetic field anomalies to enhance lineaments for the CET analyses. The lineation detection filter place lines on the edges of the enhanced linear features automatically.

A threshold is set for the amplitude of the derivative derived field to limit the number and extent of the final lineaments to be considered from the individual edge detection methods. Through a process of vectorization, lines are placed on all possible linearized geological structures for further analyses. The CET analyses map out lineament at the maximum field location of the horizontal and vertical derivatives but at the maximum-minimum field boundary of the tilt derivative grid. The mapped individual lineation is combined by superposition to establish the true lineaments. The combined mapped lineaments from the CET Grid analyses were positioned closer together. The concept of Mbarga et al. (2012) was used to establish the most reliable contact locations from the combined lineaments: 1) a true contact is established at locations where the three mapped lineaments is superimposed one another 2) possible contact locations were mapped horizontal derivative lineament is isolated from that of the vertical derivative and 3) at parallel contacts, the true contact position is the vertical derivative contact and not the tilt derivative contact (Mbarga et al., 2012). The first assumption provides the best contact positions which were achieved by tracing the final lineament as a layer with ArcMap of the ArcGIS software. The second condition satisfies the assumptions of the horizontal derivative theory (Phillips, 1998).

3.2.4. Mapped Basement Geological Structure

The basement geological structural map of the study area is shown in **Figure 7**. The mapped geological structures include linearized and curvilinear structures. The linearized structures are probably faulting and dykes-like intrusion of volcanic sources while the curvilinear structure are geological boundaries which distinguishes the various rock types in the area. The area is covered by three rock types which include metasedimentary rocks to the west, the volcaniclastics which are centrally located and the metavolcanics which occupy the east of the study area. The two major litho-contacts are labelled "L1" and "L2". The contact "L1" Separate the metasediments and volcaniclastics and the contact "T2" separate the volcaniclastics from the metavolcanics. The linearized structures are interpreted as dykes associated with various volcanic intrusions in the study area. They were grouped into major and minor dykes based on their extent, orientation and size of deposition. The major dyke labelled "D1" run through the entire study area in a northeast-southwest orientation. The minor dykes labelled "D2" to "D8" are associated with some of the major volcanic intrusions in the study area. The mapped lineaments are generally oriented in the northeast-southwest direction which is consistent with the structural trends in the Birimian Supergroup of Ghana. The underlying geological structure revealed a highly tectonized basement characterized by extensive shearing associated with basement dykes and volcanic intrusions.

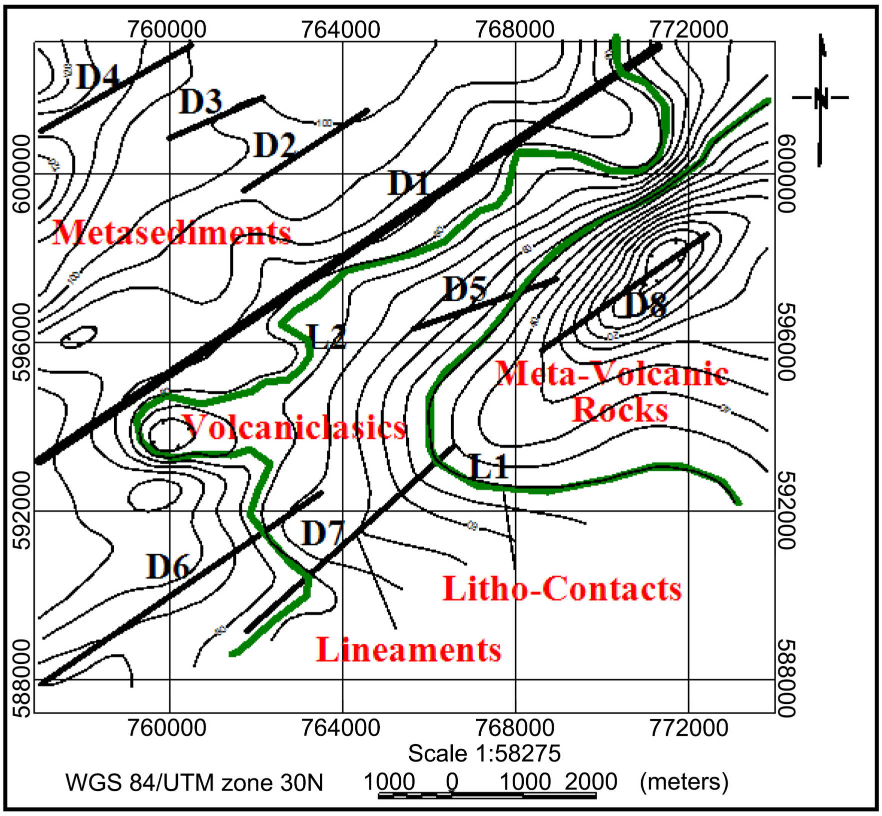

Figure 7. Basement structural map of the study area showing mapped lineaments and litho-contacts.

3.3. Advance Source Parameter Imaging (ASPI)

The relative spatial depth solution values plot (Figure 8) shows a depth range of less than 150 m to >300 m. The study area showed a varied depth distribution. The Source Parameter Imaging (SPI) technique estimates depths to magnetic-source across an area. To estimate depths to the crystalline basement, the total magnetic field intensity (TMI) grid reduced to pole was separated into a residual and regional field intensities. The SPI depths were then estimated using the regional magnetic field intensity grid. The estimated depths to magnetic sources in this geological setting using the regional magnetic field intensities were interpreted as the depths to the crystalline basement or overburden thickness because they corresponded to previous overburden drilling depths within the study area. Depth to the basement crystalline rocks increases from the northwest to the southeast, as one approaches the shoreline. This is demonstrated by the continual variation in depth solution value colours from blue to red. Deeper depths (>300 m) are shown in red depth solutions while much shallower depth (less than 150 m) solutions are shown in blue solution. The intermediate depth (150 m - 300 m) solution occurs in both yellow and green colours. The cumulative average range depth measure to the underlying crystalline basement rocks across the study area is between 150 m to 200 m shown in green colour. This depth range values formed the highest number of depth solutions across the study area. The shallower depth solution values in blues (less than 150 m) mostly occur along linearized bodies interpreted as geological dykes which occur closer to the surface. The derived deeper depth solution values (>300 m) in red occupy the southeastern part of the study area, where the metavolcanics occur. From the depth estimates, it can be concluded that the overburden rocks in the study area is approximately between 150 m - 300 m thicker in most parts of the study area except the southeast, where much thicker sediments occur along the shoreline. The Advance Source Parameter Imaging Method measured relative depth solutions values to the overburden thickness at different location within the study area (Table 1). The measured depth solution values at various location is given alongside their geographical coordinates in X and Y. The highest estimated depth solution value in the study area is 753 m at the geographical coordinates X = 768700 and Y = 592700. The measured depth solution values are important for establishing mine drilling parameters, geohazard analysis study and are considered during mine development planning.

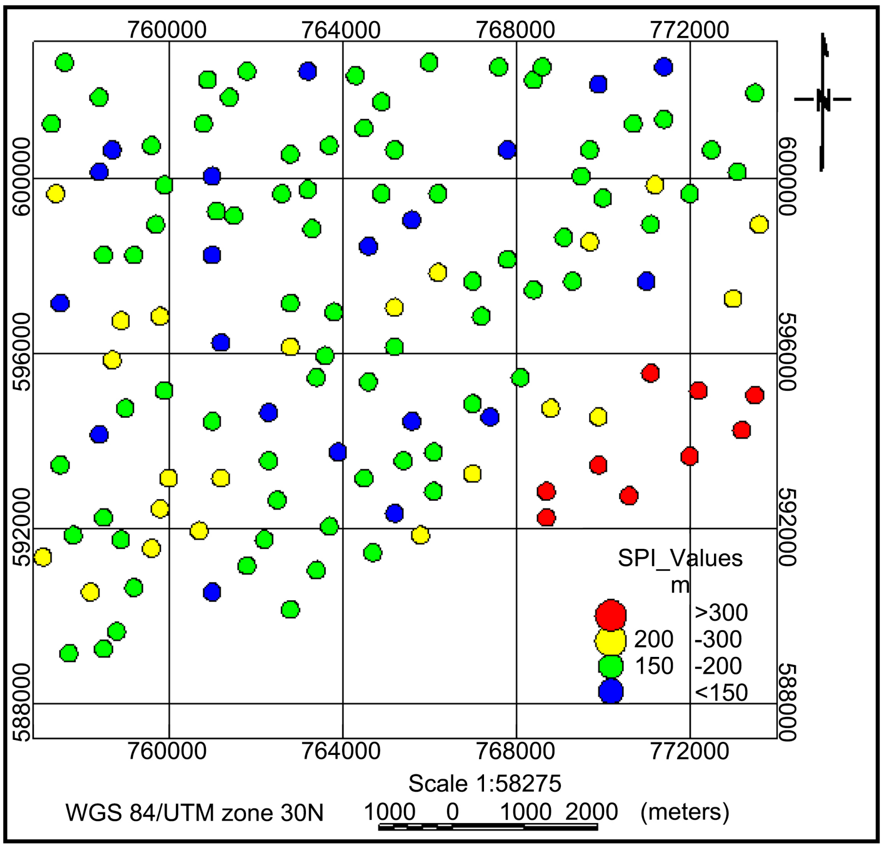

Figure 8. Advanced source parameter imaging depth solution map of the study area.

Table 1. Estimated depth solution values of the study area.

X	Y	DEPTH (m)
757,100	591,200	218
764,700	591,300	150
759,600	591,400	204
758,900	591,600	185
762,200	591,600	180
757,800	591,700	172
768,700	**592,700**	**753**
765,800	591,700	201
760,700	591,800	225
763,700	591,900	157
758,500	592,100	186
768,700	592,100	696

4. Discussion

The study focuses on mapping the geological structures and measuring depth to the overburden thickness in the Winneba area, southern Ghana. Aeromagnetic data was used to distinguish the geology of the study area into metasedimentary, metamorphosed volcaniclastics and metavolcanic rocks. The mapped areas of high magnetic intensity anomaly were correlated to the metavolcanics of the basement crystalline rocks, the intermediate magnetic anomaly intensities corresponded to the metamorphosed volcaniclastics while the low magnetic intensity anomaly areas were interpreted as the overlying metasedimentary units. A review of the magnetic anomaly distribution to the geology of the Winneba area, indicates the observed high magnetic anomaly areas correlates with the solid basement rocks of the Dahomeyide belt, which are mostly metamorphosed granitic gneisses with possible higher magnetic minerals. The measured lower anomalies corresponded to areas occupied by the overlying metasedimentary rocks of the Birimian Supergroup which are mostly meta-arenites and meta-argillites. The modeled intermediate anomalies lie between the metavolcanics and metasedimentary rocks, interpreted as the volcaniclastics which are mostly quartzites and schist.

Basement structural mapping is important in mineral exploration since most precious minerals originates from hydrothermal fluids which are associated with geological structures. Geological structures were mapped using the CET analytical method on the edge detection techniques. These are mostly lineaments trending northeast-southwest and interpreted as volcanic dykes associated with the volcanic intrusives in the study area. They include a major dyke running through the whole study area and minor once mostly associated with the volcanic rocks. The dykes are important possible sources of mineralization in the Birimian terrane of Ghana where they occur as stockworks of veins. Also mapped are distinct sets of litho-contacts forming the boundaries of the major rock types in the study area. They are the tectonized contacts between the Dahomeyan structural unit and the Birimian volcaniclastics. Geological boundaries are areas of extensive shearing and fracturing constituting a zone of weakness for fluid accumulation. The mapped geological structures are there a source of interest in for hydrothermal and structurally controlled deposits of economic importance. The SPI technique applied estimated depths to the crystalline basement or overburden thickness across the study area. The regional magnetic field intensity map was used to estimate the depths to magnetic sources which agreed with past overburden drilling depths at the study area. The measured depths to the overburden thickness show variations in material thickness across the entire study area. On an average range, the material thickness ranges between 150 m to 300 m. Deeper depths occur to the southeast and increases further southward. The estimated depth is a valuable information in mineral resource assessment and evaluation. Mineral exploratory drill parameters are planned around these estimates for optimum depth determination. In cases of overburden ore deposits, it is incorporated in the estimation procedure. Generally, depths to the crystalline basement rocks increases from the northwest, within the Birimian to the southeast where the Dahomeyan structural unit occur. The observed magnetic anomaly orientations, structural trends and depth directional variations, shows that the study area has undergone extensive tectonic activities, which has affected the basement structural configuration.

5. Conclusion

The study sought to mapped out the geological basement structure of the Winneba area and estimate depth to the overburden thickness for mineral exploration purpose. Modern geophysical techniques were used which include the CET Grid Analysis for lineament mapping and the Advanced Source Parameter Imaging for depth to magnetic sources measurement. The methods were effective in mapping geological structures and estimating spatial depths across the study area. The study established the principal rocks in the area as metamorphosed sedimentary, volcaniclastics and volcanic rocks. The high magnetic anomalies correlated to the metavolcanic rocks, the intermediate magnetic anomalies corresponded to the metamorphosed volcaniclastics and the low magnetic anomalies areas were interpreted as metasedimentary rocks. The mapped geological structures were linearized dykes and curvilinear litho-contacts. The delineated dykes include major and minor types based on their sizes and linear extent. Measured depths solution to the underlying regional rocks showed variations in material thickness over the study area. Deeper depths greater than 300 m occur to the southeast while much shallower depths less than 150 m were along the position of isolated central dykes. Intermediate depths (150 m - 300 m) were measured across the entire study area.

An average range depth measure to the underlying crystalline basement rocks across the study area is approximated between 150 m to 200 m. From, the depths measurement, the overburden material is thicker to the southeast compared to the central and northwestern parts of the study area. The highest estimated depth is 753 m located southeast. The study proposed the mapped litho-contacts and intruded dyke locations as probable zones of mineralization for further exploration works.

Author Contributions

Conceptualization, methodology, validation, formal analysis, investigation, original draft preparation, review and editing, proofreading and visualization. All the above were done by Daniel Oduro Boatey Nuamah.

Conflicts of Interest

The author declare no conflicts of interest regarding the publication of this paper.

References

Affaton, P., Rahaman, M. A., Trompette, R., & Sougy, J. (1991). The Dahomeyide Orogen: Tectonothermal Evolution and Relationships with the Volta Basin. In R. D. Dallmeyer, & J. P. Lécorché (Eds.), *The West African Orogens and Circum-Atlantic Correlatives* (pp. 107-122). Springer Berlin. https://doi.org/10.1007/978-3-642-84153-8_6

Akulga, A. (2013). Structural Controls on Gold Mineralization in Birimian Terrains of Ghana. *International Journal of Geosciences, 37,* 1-13.

Anum, S., Sakyi, P. A., Su, B., Nude, P. M., Nyame, F., Asiedu, D. et al. (2015). Geochemistry and Geochronology of Granitoids in the Kibi-Asamankese Area of the Kibi-Winneba Volcanic Belt, Southern Ghana. *Journal of African Earth Sciences, 102,* 166-179. https://doi.org/10.1016/j.jafrearsci.2014.11.007

Attoh, K., Dallmeyer, R. D., & Affaton, P. (1997). Chronology of Nappe Assembly in the Pan-African Dahomeyide Orogen, West Africa: Evidence from Mineral Ages. *Precambrian Research, 82,* 153-171. https://doi.org/10.1016/s0301-9268(96)00031-9

Castaing, C., Triboulet, C., Feybesse, J. L., & Chèvremont, P. (1993). Tectonometamorphic Evolution of Ghana, Togo and Benin in the Light of the Pan-African/Brasiliano Orogeny. *Tectonophysics, 218,* 323-342. https://doi.org/10.1016/0040-1951(93)90322-b

Forson, E. D., Menyeh, A., & Wemegah, D. D. (2021). Mapping Lithological Units, Structural Lineaments and Alteration Zones in the Southern Kibi-Winneba Belt of Ghana Using Integrated Geophysical and Remote Sensing Datasets. *Ore Geology Reviews, 137,* Article ID: 104271. https://doi.org/10.1016/j.oregeorev.2021.104271

Forson, E. D., Menyeh, A., Wemegah, D. D., Danuor, S. K., Adjovu, I., & Appiah, I. (2020). Mesothermal Gold Prospectivity Mapping of the Southern Kibi-Winneba Belt of Ghana Based on Fuzzy Analytical Hierarchy Process, Concentration-Area (C-A) Fractal Model and Prediction-Area (P-A) Plot. *Journal of Applied Geophysics, 174,* Article ID: 103971. https://doi.org/10.1016/j.jappgeo.2020.103971

Ganade, C. E., Cordani, U. G., Agbossoumounde, Y., Caby, R., Basei, M. A. S., Weinberg, R. F. et al. (2016). Tightening-Up NE Brazil and NW Africa Connections: New U-Pb/Lu-Hf Zircon Data of a Complete Plate Tectonic Cycle in the Dahomey Belt of the West Gondwana Orogen in Togo and Benin. *Precambrian Research, 276,* 24-42. https://doi.org/10.1016/j.precamres.2016.01.032

Groves, D. I., Goldfarb, R. J., Robert, F., & Hart, C. J. R. (2003). Gold Deposits in Metamorphic Belts: Overview of Current Understanding, Outstanding Problems, Future Research, and Exploration Significance. *Economic Geology, 98,* 1-29. https://doi.org/10.2113/gsecongeo.98.1.1

Hinze, W. J., von Frese, R. R. B., & Saad, A. H. (2013). *Gravity and Magnetic Exploration: Principles, Practices, and Applications.* Cambridge University Press. https://doi.org/10.1017/cbo9780511843129

Hirdes, W., Davis, D. W., & Eisenlohr, B. N. (1992). Reassessment of Proterozoic Granitoid Ages in Ghana on the Basis of U/Pb Zircon and Monazite Dating. *Precambrian Research, 56,* 89-96. https://doi.org/10.1016/0301-9268(92)90085-3

Ilesanmi, K. S., Tata, H., Nzelibe, I. U., & Idowu, T. O. (2025). Multi-Resolution Analysis of Gravity Anomalies: A Comparative Study of Modern and Spherical Approximation Techniques. *Nova Geodesia, 5,* Article 337. https://doi.org/10.55779/ng53337

Kovačević, M. S., Marčić, D., and Gazdek, M. (2018). Application of Geophysical Investigations in Underground Engineering. *Gradevinar, 70,* 1111-1117.

Lowrie, W. (2007). *Fundamentals of Geophysics* (2nd ed.). Cambridge University Press. https://doi.org/10.1017/cbo9780511807107

Mbarga, T. N., Feumoe, A. N. S., Dicoum, E., & Fairhead, J. D. (2012). Aeromagnetic Data Interpretation to Locate Buried Faults in South-East Cameroon. *Geophysical Journal, 48,* 49-63.

Nabighian, M. N. (1972). The Analytic Signal of Two-Dimensional Magnetic Bodies with Polygonal Cross-Section; Its Properties and Use for Automated Anomaly Interpretation. *Geophysics, 37,* 507-517. https://doi.org/10.1190/1.1440276

Nabighian, M. N., Grauch, V. J. S., Hansen, R. O., LaFehr, T. R., Li, Y., Peirce, J. W. et al. (2005). 75th Anniversary: The Historical Development of the Magnetic Method in Exploration. *Geophysics, 70,* 33ND-61ND. https://doi.org/10.1190/1.2133784

Phillips, J. D. (1998). *Processing and Interpretation of Aeromagnetic Data for the Santa Cruz Basin—Patahonia Mountains Area, South-Central Arizona.* U.S. Geological Survey Open-File Report, Arizona, 02-98.

Pigois, J. P., Groves, D. I., Fletcher, I. R., McNaughton, N. J., & Snee, L. W. (2003). Age Constraints on Tarkwaian Palaeoplacer and Lode-Gold Formation in the Tarkwa-Damang District, SW Ghana. *Mineralium Deposita, 38,* 695-714. https://doi.org/10.1007/s00126-003-0360-5

Smith, R. S., Thurston, J. B., Dai, T. F., & MacLeod, I. N. (1998). ISPI™—The Improved Source Parameter Imaging Method. *Geophysical Prospecting, 46,* 141-151. https://doi.org/10.1046/j.1365-2478.1998.00084.x

Taylor, P. N., Moorbath, S., Leube, A., & Hirdes, W. (1992). Early Proterozoic Crustal Evolution in the Birimian of Ghana: Constraints from Geochronology and Isotope Geochemistry. *Precambrian Research, 56,* 97-111. https://doi.org/10.1016/0301-9268(92)90086-4

Telford, W. M., Geldart, L. P., & Sheriff, R. E. (1990). *Applied Geophysics* (2nd ed.). Cambridge University Press. https://doi.org/10.1017/cbo9781139167932

Thurston, J. B., & Smith, R. S. (1997). Automatic Conversion of Magnetic Data to Depth, Dip, and Susceptibility Contrast Using the SPI (TM) Method. *Geophysics, 62,* 807-813. https://doi.org/10.1190/1.1444190

Verduzco, B., Fairhead, J. D., Green, C. M., & MacKenzie, C. (2004). New Insights into Magnetic Derivatives for Structural Mapping. *The Leading Edge, 23,* 116-119. https://doi.org/10.1190/1.1651454